

The Fault-Tolerant Control of Magnetic Bearings With Reduced Controller Outputs

Uhn Joo Na

Research Engineer
e-mail: ujn2738@acs.tamu.edu

Alan Palazzolo

Professor

Texas A&M University,
Mechanical Engineering,
College Station, TX 77843-3123

The fault-tolerant control scheme utilizes grouping of currents to reduce the required number of controller outputs. Reduced current distribution matrices can be calculated with the constraint conditions of the controller outputs and the necessary condition for linearization. Decoupling chokes are not required for the control scheme with grouped currents since fluxes are isolated in C-cores. By reducing controller outputs and removing decoupling chokes the fault-tolerant control scheme is more efficient and practical in terms of industrial applications. [DOI: 10.1115/1.1369356]

1 Introduction

Magnetic bearings are filling greater applications in industry since they have many advantages over conventional fluid film bearings such as elimination of lubrication, less power loss, and operations at temperature extremes. Furthermore, active stiffness and damping properties of magnetic bearings make it possible to adjust rotordynamic properties while operating the rotor-bearing system. Synchronous vibration due to imbalance can also be successfully reduced by automatic balancing [1]. The modeling and design of magnetic bearings have been investigated by many researchers [2–4]. However, reliability requirements limit magnetic bearings from being used in many potential applications. Fault tolerant control of heteropolar magnetic bearings has been investigated by several researchers to improve reliability.

Maslen and Meeker [5] developed a fault-tolerant control scheme of a 8-pole heteropolar magnetic bearing with independently controlled currents. Their approach utilizes the flux coupling property of heteropolar magnetic bearings. Redefining remaining coil currents with the distribution matrix, when one or more coils are disconnected, makes it possible to produce desired force resultants with the help of flux coupling. However, flux coupling with independent currents results in an electromagnetic stability problem. Current states become unstable because one of the eigenvalues of the rank-deficient inductance matrix is zero, which results in power amplifier limiting [6]. Meeker [6] introduced the decoupling choke to remedy this stability problem. In essence, to use a decoupling choke means that all coils from the magnetic bearing are wound around a common, external electromagnet core, then return to their power amplifiers. The number of coil turns in the decoupling choke can be designed to produce additional inductance so that the inductance matrix should be completely nonsingular. The fault-tolerant magnetic bearings were demonstrated on a large flexible rotor [7].

This fault-tolerant control scheme has an advantage over the 3 control-axis redundant control scheme developed by Lyons [8] with regard to fault tolerance of multiple failed poles. The 3 control-axis redundant control scheme will not work if 2 of the 3 control axes experience any number of coil failures. This advantage of the former over the latter approach does require an increase in hardware complexity for implementation. The fault-tolerant control scheme of an 8-pole heteropolar magnetic bearing with independently controlled currents requires 8 digital controller output channels while the 3 control-axis redundant control scheme requires only 3 digital controller output channels. Therefore, 16

output channels are required for the control of 2 redundant radial bearings. Furthermore, a decoupling choke is required for each bearing. This requirement for extensive hardware may prevent the control scheme from being used in some industrial applications.

Reducing the number of digital controller outputs and eliminating decoupling chokes make the fault tolerant control scheme more practical for industrial applications. Fault tolerant schemes that only require 3 controller outputs for a radial bearing may be implemented on a commercial 8-channel DSP controller for fault tolerant control of a five-axis rotor-bearing system.

2 Fault Tolerance of Grouped Magnetic Bearings

Fluxes can be isolated for a multiple-pole magnetic bearing when coils are wound in series with a second pole of opposite polarity. Figure 1 shows that control currents of the 12-pole heteropolar magnetic bearing can be separated into 3 groups (6 coil pairs, where a coil pair is two coils wound in series on different poles). The flux vector of the 1-D magnetic circuit is [5]

$$\phi(x, y) = R(x, y)^{-1} N I = V(x, y) I \quad (1)$$

where R , N , and I represent the reluctance matrix, coil turn matrix, and the current vector, respectively. The current vector with coil coupling is

$$I = N_I \hat{I} \quad (2)$$

where the coil coupling matrix for the 12-pole bearing is

$$N_I = \begin{bmatrix} -1 & 0 & 0 & 0 & 0 & 0 \\ 0 & -1 & 0 & 0 & 0 & 0 \\ 0 & 1 & 0 & 0 & 0 & 0 \\ 0 & 0 & 1 & 0 & 0 & 0 \\ 0 & 0 & -1 & 0 & 0 & 0 \\ 0 & 0 & 0 & -1 & 0 & 0 \\ 0 & 0 & 0 & 1 & 0 & 0 \\ 0 & 0 & 0 & 0 & 1 & 0 \\ 0 & 0 & 0 & 0 & -1 & 0 \\ 0 & 0 & 0 & 0 & 0 & -1 \\ 0 & 0 & 0 & 0 & 0 & 1 \\ 1 & 0 & 0 & 0 & 0 & 0 \end{bmatrix}$$

The flux vector evaluated at the bearing center position is

$$\phi_{\left. \begin{matrix} x=0 \\ y=0 \end{matrix} \right\}} = \frac{n a \mu_0}{g_0} N_I \hat{I} \quad (3)$$

where a , μ_0 , g_0 , and n represent pole face area, permeability of air, nominal air gap, and number of coil turns, respectively. Equation (3) shows that all fluxes are isolated in C cores (equal magnitude and opposite polarity type paths). Note that the 6 C-core

Contributed by the Dynamic Systems and Control Division for publication in the JOURNAL OF DYNAMIC SYSTEMS, MEASUREMENT, AND CONTROL. Manuscript received by the Dynamic Systems and Control Division March 24, 2000. Associate Editor: J. Tu.

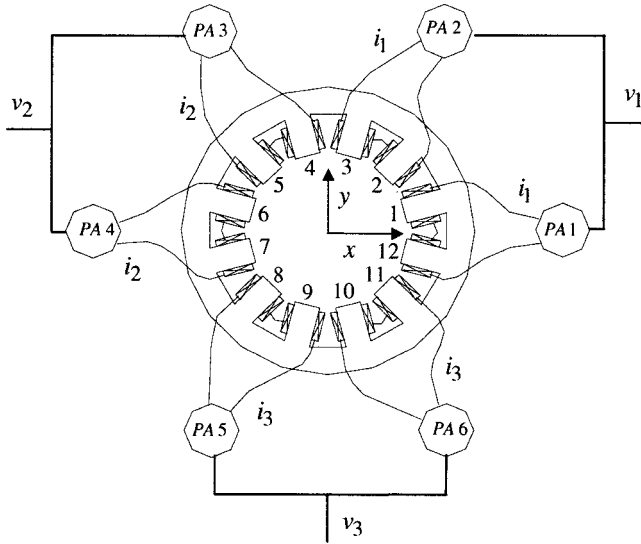


Fig. 1 Heteropolar magnetic bearing with grouped currents

fluxes can be controlled by their independent power amplifiers. The electric circuit equation for the power amplifiers loads is

$$L(x, y) \frac{\partial \hat{I}}{\partial t} + \mathfrak{R} \hat{I} = V_s \quad (4)$$

where the inductance matrix evaluated at the bearing center position is given as

$$L_{|x=y=0} = \frac{n^2 a \mu_0}{g_0} N_I^T N_I$$

$$H = \begin{bmatrix} -1 & -1 & 1 & 0 & 0 & 0 & 0 & 0 & 0 & 0 & 0 & 1 \\ 0 & 0 & 0 & 1 & -1 & -1 & 1 & 0 & 0 & 0 & 0 & 0 \\ 0 & 0 & 0 & 0 & 0 & 0 & 0 & 1 & -1 & -1 & 1 & 0 \end{bmatrix}^T, \quad I_0 = [i_1, i_2, i_3]^T$$

The matrix H is also used to define the grouping of currents with the multiple coils failed bearing. For example, H for 2-3-6-7th poles (2-4th coils) failed bearing is given as

$$H = \begin{bmatrix} -1 & 0 & 0 & 0 & 0 & 0 & 0 & 0 & 0 & 0 & 0 & 1 \\ 0 & 0 & 0 & 1 & -1 & 0 & 0 & 0 & 0 & 0 & 0 & 0 \\ 0 & 0 & 0 & 0 & 0 & 0 & 0 & 1 & -1 & -1 & 1 & 0 \end{bmatrix}^T \quad (9)$$

The control current output vector I_0 is defined as

$$I_0 = \kappa T V_c \quad (10)$$

where

$$V_c = [v_b, v_{cx}, v_{cy}]^T$$

and where κ represents the power amplifier's DC gain. v_b , v_{cx} , and v_{cy} are bias, x control, and y control voltage outputs, respectively. The distribution matrix T is defined as

$$T = [T_b, T_x, T_y] \quad (11)$$

where

$$T_b = [t_1, t_2, t_3]^T, \quad T_x = [t_4, t_5, t_6]^T, \quad T_y = [t_7, t_8, t_9]^T$$

and \mathfrak{R} and V_s represent resistance matrix and voltage source vector, respectively. The inductance matrix is completely decoupled and nonsingular because $N_I^T N_I$ is diagonal.

The force-current relationship of a heteropolar magnetic bearing has been investigated by many researchers [9-11]. Leakage and fringing effects can be approximated by a simple derate factor [12]. The flux density vector in the air gap with the leakage and fringing effects is

$$B = \frac{\sigma}{a} VI \quad (5)$$

where σ represents the leakage and fringing factor. Magnetic forces are determined from

$$F_\varphi = -B^T \frac{\partial D}{\partial \varphi} B \quad (6)$$

where the air gap energy matrix is

$$D = \text{diag}(g_j a / (2\mu_0)) \quad (7)$$

and where g_j represents the air gap of the j th pole, and φ is either x or y .

Constraint conditions are applied on the controller voltage outputs in a manner such that any coil in a group has the same current as any other coil in its group. The same control voltages are applied to the two power amplifiers of each group of 4 adjacent poles so that only 3 independent currents are required. The current vector to the unfailed bearing is related to the control output current vector by defining a map matrix H .

$$I = H I_0 \quad (8)$$

where

The current distribution matrix T must be determined so that magnetic forces in the grouped bearing are linearized and decoupled even in case of multiple coils failed. The necessary conditions for force linearization and uncoupling are [5,13]

$$T^T G_\varphi T = M_\varphi \quad (12)$$

where

$$G_\varphi = -H^T V^T \frac{\partial D}{\partial \varphi} V H$$

$$M_x = \begin{bmatrix} 0 & 0.5 & 0 \\ 0.5 & 0 & 0 \\ 0 & 0 & 0 \end{bmatrix}, \quad M_y = \begin{bmatrix} 0 & 0 & 0.5 \\ 0 & 0 & 0 \\ 0.5 & 0 & 0 \end{bmatrix}$$

To yield the linearized forces;

$$F_\varphi = v_b v_{c\varphi} \quad (13)$$

If there exists a distribution matrix T that satisfies Eq. (12) for a specific failure case, a set of 3 independent currents will be distributed into 3 groups of poles to produce desired force resultants in the x and y directions.

This bearing with 3 groups of independent currents works like three independent force sources. One of the two C-cores in each group is redundant, and will be completely shut down if its coil pair fails. Following this event, a new set of three adaptive currents will be distributed to the failed bearing to produce the desired force resultants. However, the system will fail if both C-cores in any group fail since at least 3 independent currents are required to generate arbitrary forces in a magnetic bearing [6]. Distribution matrices can be calculated for the bearing up to 3 coil pairs failed out of 6 coil pairs, with a requirement that at least one unfailed coil pair exist in each group. This 12-pole/6-coil pair grouping strategy has more coil redundancy than the 3 control-axis method suggested by Lyons et al. [8]. Their 12-pole/3 control-axis redundant control scheme will not work if 2 of the 3 control axes experience any number of coil failures.

If a 16-pole bearing with 4 groups and 8 C-cores is used, one of the 4 groups is redundant. The 4×3 distribution matrices can be calculated for the bearing with 3 adjacent coil pairs failed, or up to 5 coil pairs failed out of 8 coil pairs at the cost of one more controller output (total 4).

3 Determination of Distribution Matrices

The distribution matrices for the fault-tolerant bearing with reduced control outputs are calculated by using a Lagrange Multiplier optimization method. The cost function of the weighted norm of the flux density vector is

$$J(T) = B(T)^T P B(T) = I^T V^T P V I \quad (14)$$

Subject to the equality constraints (12)

$$T^T G_\varphi T - M_\varphi = 0 \quad (15)$$

Although a diagonal weighting matrix P can be assigned to increase load capacity in a specific direction, an identity matrix is selected here for simplicity. Twelve equality constraint equations are derived from Eqs. (15) with $\varphi \in (x, y)$

$$\begin{aligned} h_1(T) &= T_b^T G_x T_b = 0 \\ h_2(T) &= T_b^T G_x T_x - 0.5 = 0 \\ h_3(T) &= T_b^T G_x T_y = 0 \\ h_4(T) &= T_x^T G_x T_x = 0 \\ h_5(T) &= T_x^T G_x T_y = 0 \\ h_6(T) &= T_y^T G_x T_y = 0 \\ h_7(T) &= T_b^T G_y T_b = 0 \\ h_8(T) &= T_b^T G_y T_x = 0 \\ h_9(T) &= T_b^T G_y T_y - 0.5 = 0 \\ h_{10}(T) &= T_x^T G_y T_x = 0 \\ h_{11}(T) &= T_x^T G_y T_y = 0 \\ h_{12}(T) &= T_y^T G_y T_y = 0 \end{aligned} \quad (16)$$

The Lagrange Multiplier method is applied to the problem of solving for the T that satisfies Eq. (12). Define:

$$\hat{L}(T) = J(T) + \sum_{j=1}^{12} \lambda_j h_j(T) \quad (17)$$

where λ_j are Lagrange multipliers. Partial differentiation of Eq. (17) with respect to t_i and λ_j leads to 21 nonlinear algebraic equations to solve for t_i and λ_j .

$$w_i = \frac{\partial \hat{L}}{\partial t_i} = 0, \quad i = 1, 2, \dots, 9 \quad (18)$$

$$w_{j+9} = h_j(T) = 0, \quad j = 1, 2, \dots, 12 \quad (19)$$

The vector form of these equations is

$$W t, \lambda = \begin{bmatrix} w_1(t, \lambda) \\ w_2(t, \lambda) \\ \vdots \\ w_{20}(t, \lambda) \\ w_{21}(t, \lambda) \end{bmatrix} = \begin{bmatrix} 0 \\ 0 \\ \vdots \\ 0 \\ 0 \end{bmatrix} \quad (20)$$

The distribution matrices T 's are calculated by solving the system of nonlinear algebraic equations shown in Eq. (20). A nonlinear algebraic equation solver using a least square iterative method (MATLAB) was used to solve Eq. (20) numerically. Various initial guesses of t_i and λ_j are used in order to find the converged solutions. The 12-pole heteropolar magnetic bearing used in this analysis has uniform pole face area a of $1.6058 \times 10^{-4} \text{ m}^2$, a nominal gap g_0 of $5.08 \times 10^{-4} \text{ m}$, and number of coil turns n of 100. The distribution matrix T is always a 3×3 matrix for any failure case in this "3 group" strategy.

Several distribution matrices were calculated for the unfailed and failed bearings. A valid T matrix for a 12-pole/3 group heteropolar magnetic bearing in unfailed coil operation is given as

$$T_u = \begin{bmatrix} 0.45108 & 0.0488 & 0.03385 \\ 0.45108 & -0.049 & 0.033825 \\ -0.45108 & 0.000075 & 0.050875 \end{bmatrix} \quad (21)$$

A distribution matrix for the 2 coil pairs failed bearing (2–4th coil pairs failed) is

$$T_2 = \begin{bmatrix} 0.36694 & 0.10825 & 0.041664 \\ 0.51893 & -0.10205 & 0.058921 \\ 0.36694 & -0.072163 & -0.0662496 \end{bmatrix} \quad (22)$$

A distribution matrix for the 3 coil pairs failed bearing (2–4–6th coil pairs failed) is

$$T_3 = \begin{bmatrix} 0.93579 & 0.054469 & 0.081712 \\ 0.93579 & -0.054421 & 0.081712 \\ -0.4679 & 0 & 0.10061 \end{bmatrix} \quad (23)$$

4 Control System Design

The calculated distribution matrices, which work like adaptive gain matrices to compensate for missing coils, can be implemented in a physical controller, so if some combinations of failures of the power amplifiers or coils are detected, the corresponding distribution matrices can be switched shortly thereafter. Figure 2 shows a diagram for illustrating the operation of the fault-tolerant controller. The inputs are the 2 position signals and the reference bias voltage v_b . Both control gains and distribution matrices must be adjusted for the specific configuration of coil failures. This fault-tolerant scheme only requires 3 DSP controller outputs for a radial bearing, so a commercial 8-channel DSP controller can be used for the fault tolerant control of a five-axis rotor-bearing system.

The nonlinear magnetic force in Eq. (6) can be linearized about the bearing center position and the zero control voltages by using Taylor series expansion [13,14]. The bias voltage gain can be adjusted for the given distribution matrix so that the maximum component of the bias flux density vector is equal to $b_{sat}/2$, to generate maximum load. The parameter b_{sat} represents the saturation flux density. The linearized forces are

$$F_x = -K_{p_{xx}}x - K_{p_{xy}}y + K_{v_{xx}}v_{cx} \quad (24)$$

$$F_y = -K_{p_{yx}}x - K_{p_{yy}}y + K_{v_{yy}}v_{cy} \quad (25)$$

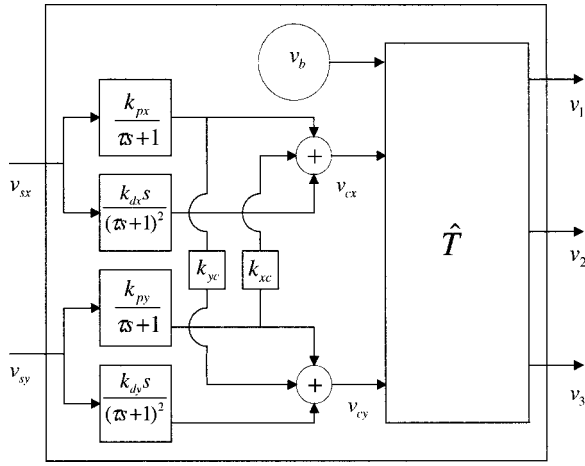


Fig. 2 Fault-tolerant control scheme with 3 coil groups

The position stiffnesses are described as

$$K_{p\varphi\omega} = -\sigma^2 \kappa^2 T_b^T H^T U_{\varphi\omega 0} H T_b v_b^2 \quad (26)$$

and voltage stiffnesses are described as

$$K_{v\varphi\omega} = 2\sigma^2 \kappa^2 T_b^T H^T U_{\varphi 0} H T_b v_b \quad (27)$$

where

$$U_{\varphi 0} = -V \frac{\partial D}{\partial \varphi} V^T \Big|_{\varphi=0}, \quad U_{\varphi\omega 0} = -2V \frac{\partial D}{\partial \varphi} \left(\frac{\partial V}{\partial \omega} \right)^T \Big|_{\varphi=0, \omega=0}$$

and where both φ and ω represent either x or y . The position stiffnesses and voltage stiffnesses are calculated for the distribution matrices of T_u and T_2 for the given bias voltages as shown in Table 1.

The simple PD control with low pass filters are used to design the closed-loop system for unfailed bearings. The closed-loop dynamic properties can be calculated when the control gains are appropriately selected [15]. The same closed-loop stiffnesses and dampings may be maintained before and after coil failure if control gains are switched to appropriate values. The decoupled linearized forces for an unfailed bearing are

$$F_x^N = -K_{p\varphi\varphi}^N \varphi + K_{v\varphi\varphi}^N v_{c\varphi} \quad (28)$$

where

$$v_{c\varphi}^N = -k_{p\varphi}^N v_{s\varphi} - k_{d\varphi}^N \dot{v}_{s\varphi}, \quad v_{s\varphi} = \xi \varphi$$

and where ξ is the sensor sensitivity. In general, the linearized forces for the failed bearing have undesirable cross-coupled position stiffnesses, and the direct position stiffnesses along the x and y axes are usually not symmetric. Cross feedback control forces are added in the linearized force equations of the failed bearing in order to cancel out the cross coupled position stiffnesses. The linearized forces for the failed bearing are

$$F_x^F = -K_{p_{xx}}^F x - K_{p_{xy}}^F y + K_{v_{xx}}^F (v_{cx}^F + \hat{v}_{cx}) \quad (29)$$

Table 1 The calculated stiffnesses

	T_u	T_2
v_b	5	5
$K_{p_{xx}}$ (N/m)	-469800	-212460
$K_{p_{xy}}$ (N/m)	0	78721
$K_{p_{yx}}$ (N/m)	0	78721
$K_{p_{yy}}$ (N/m)	-462800	-303360
$K_{v_{xx}}, K_{v_{yy}}$ (N/Volt)	5	5

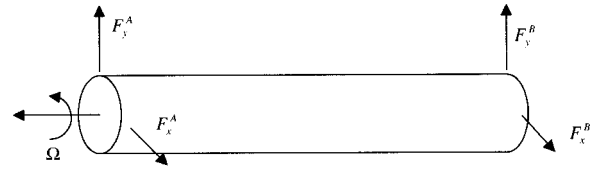


Fig. 3 Schematic of the rotor-bearing system

$$F_y^F = -K_{p_{yx}}^F x - K_{p_{yy}}^F y + K_{v_{yy}}^F (v_{cy}^F + \hat{v}_{cy}) \quad (30)$$

where

$$v_{c\varphi}^F = -k_{p\varphi}^F v_{s\varphi} - k_{d\varphi}^F \dot{v}_{s\varphi}$$

$$\hat{v}_{cx} = -k_{yc} k_{p_x}^F v_{sx}, \quad \hat{v}_{cy} = -k_{xc} k_{p_y}^F v_{sy}$$

The necessary conditions for the same closed loop stiffnesses and dampings before and after failure are

$$F_x^N = F_x^F, \quad F_y^N = F_y^F \quad (31)$$

This yields PD control gains for the failed bearing operation

$$k_{p_{xx}}^F = \frac{-K_{p_{xx}}^F + K_{p_{xx}}^N + \xi K_{v_{xx}}^N k_{p_{xx}}^N}{\xi K_{v_{xx}}^F} \quad (32)$$

$$k_{p_{yy}}^F = \frac{-K_{p_{yy}}^F + K_{p_{yy}}^N + \xi K_{v_{yy}}^N k_{p_{yy}}^N}{\xi K_{v_{yy}}^F} \quad (33)$$

$$k_{d_x}^F = \frac{K_{v_{xx}}^N}{K_{v_{xx}}^F} k_{d_x}^N \quad (34)$$

$$k_{d_y}^F = \frac{K_{v_{yy}}^N}{K_{v_{yy}}^F} k_{d_y}^N \quad (35)$$

The cross feedback gains to eliminate the cross-coupled position stiffnesses are

$$k_{xc} = -\frac{K_{p_{xy}}^F}{\xi k_{p_y}^F K_{v_{xx}}^F} \quad (36)$$

$$k_{yc} = -\frac{K_{p_{yx}}^F}{\xi k_{p_x}^F K_{v_{yy}}^F} \quad (37)$$

5 Simulations

The fault-tolerant control system is simulated for multiple coils failed cases on a horizontal rigid rotor supported with 12-pole heteropolar bearings. The schematic of the rotor-bearing system is shown in Fig. 3. The symmetric rotor used in this analysis has mass of 10 kg, polar moment of inertia of 0.05 kgm², and transverse moment of inertia of 0.2 kgm² about the mass center. Two magnetic bearings are located at 0.1 m either side of the mass center. An unbalance eccentricity e of 40×10^{-6} m for the total rotor mass is applied at both bearing locations with relative phase angle 90 deg. Power amplifier and sensor dynamics are included in the closed-loop system with a power amplifier gain κ of 1 ampere/volt and sensor sensitivity ξ of 7874 volt/m. The power amplifier dynamics is $PA(s) = 1/(\tau_p s + 1)$, where $\tau_p = 1/(2\pi f_p)$, and $f_p = 2500$ Hz. The sensor dynamics is given as $S(s) = 1/(\tau_s s + 1)$, where $\tau_s = 1/(2\pi f_s)$, and $f_s = 3000$ Hz.

The transient response from normal operation with no failure to fault-tolerant control with 2–4th coil pairs failed for both bearings was simulated for nonlinear bearings at 10,000 rpm. The selected control gains of $k_{p_{xx}}^N$, $k_{p_{yy}}^N$, $k_{d_x}^N$, and $k_{d_y}^N$ for the unfailed operation are 80, 80, 0.2 and 0.2, respectively. The required control gains of $k_{p_{xx}}^F$, $k_{p_{yy}}^F$, $k_{d_x}^F$, $k_{d_y}^F$, k_{xc} , and k_{yc} to maintain the same closed-loop dynamic properties are 73.46, 75.95, 0.2, 0.2, -0.0263, and -0.0272, respectively.

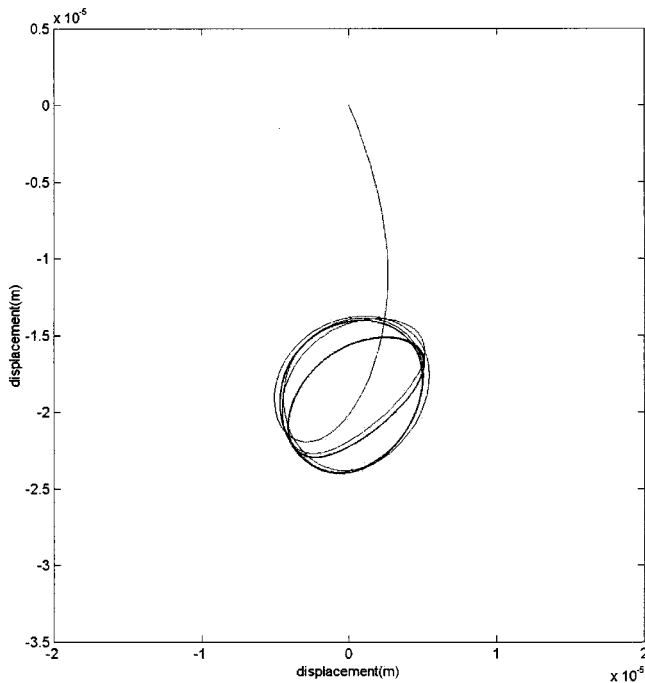


Fig. 4 Orbit plot for normal operation to the 2–4th coil pairs failed operation

Transient response of the orbit at bearing A is shown in Fig. 4. The orbit plot shows that the rotor sags slightly due to gravity and makes good orbits for normal operation. The distribution matrix of T_u was switched to T_2 when 2 coil pairs failed at 0.1 second. The orbit becomes elliptic after failure. Transient response of the current inputs to bearing A for the 2–4th coil pairs failed case is shown in Fig. 5. This shows that large amount of currents to the unfailed poles are required to maintain the similar orbits before and after failure. Transient response of the flux densities to bear-

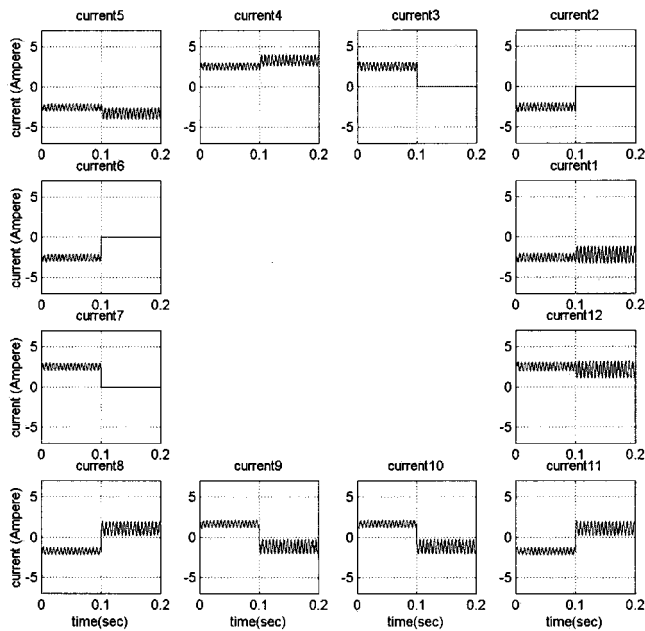


Fig. 5 Current plot for normal operation to the 2–4th coil pairs failed operation

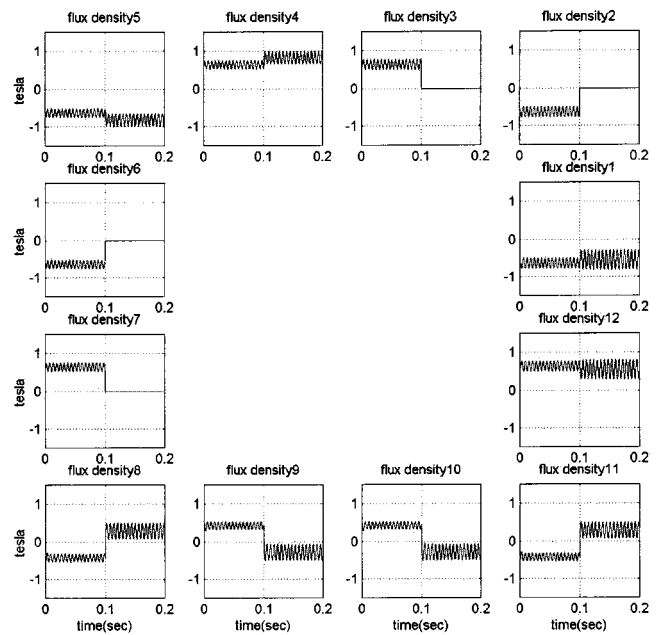


Fig. 6 Flux density plot for normal operation to the 2–4th coil pairs failed operation

ing A for the 2–4th coil pairs failed case is shown in Fig. 6. It is notable that the fluxes in 2–3–6–7th poles are completely eliminated with the distribution matrix of T_2 .

6 Conclusions

With the proposed fault-tolerant control scheme the number of required controller outputs is greatly reduced. Since this fault-tolerant scheme only requires 3 controller outputs per radial bearing, a commercial 8-channel DSP controller is sufficient to implement five-axis redundant control. Unlike the requirements of the Maslen and Meeker approach, decoupling chokes are not required for the proposed redundant control with 6 power amplifiers. The control scheme utilizes flux isolation (C core) property of heteropolar magnetic bearings. Compared to the previous approach [5] with an 8-pole bearing, this control scheme reduces controller outputs by half or more, and removes decoupling choke requirement. This will facilitate fault-tolerant control of heteropolar magnetic bearings for industrial applications. Simulations of a horizontal rigid rotor supported on two 12 pole bearings with grouped currents show that the system maintains good control even when multiple coils fail simultaneously.

Acknowledgments

The authors gratefully acknowledge the technical and funding support of this project from Albert Kascak and Gerald Montague of the U.S. Army and Andy Provenza and Ralph Jansen of NASA Glenn and the Office of NAVAL Research (Tom Calvert, Lyn Peterson, and Glenn Bell).

References

- [1] Habermann, H., and Liard, G., 1979, "Practical Magnetic Bearings," IEEE Spectr., IEEASAM Sept., pp. 26–30.
- [2] Allaire, P. E., Lewis, D. W., and Knight, J. D., 1983, "Active Vibration Control of a Single Mass Rotor on Flexible Supports," J. Franklin Inst., **315**, pp. 211–222.
- [3] Salm, J., and Schweitzer, G., 1984, "Modeling and Control of a Flexible Rotor with Magnetic Bearing," *Proceedings of the Third International Conference on Vibrations in Rotating Machinery*, pp. 553–561.
- [4] Matsumura, F., and Yoshimoto, T., 1986, "System Modeling and Control of a Horizontal-Shaft Magnetic-Bearing System," IEEE Trans. Magn., **22**, pp. 197–206.
- [5] Maslen, E. H., and Meeker, D. C., 1995, "Fault Tolerance of Magnetic Bear-

- ings by Generalized Bias Current Linearization," IEEE Trans. Magn., **31**, No. 3, pp. 2304–2314.
- [6] Meeker, D. C., 1996, "Optimal Solutions to the Inverse Problem in Quadratic Magnetic Actuators," Ph.D. dissertation, Univ. of Virginia, Mechanical Engineering.
- [7] Maslen, E. H., Sortore, C. K., Gillies, G. T., Williams, R. D., Fedigan, S. J., and Aimone, R. J., 1999, "Fault Tolerant Magnetic Bearings," ASME J. Eng. Gas Turbines Power, **121**, pp. 504–508.
- [8] Lyons, J. P., Preston, M. A., Gurumoorthy, R., and Szczesny, P. M., 1994, "Design and Control of a Fault-Tolerant Active Magnetic Bearing System for Aircraft Engine," *Proceedings of the Fourth International Symposium on Magnetic Bearings*, ETH Zurich, pp. 449–454.
- [9] Maslen, E., Hermann, P., Scott, M., and Humphris, R. R., 1989, "Practical Limits to the Performance of Magnetic Bearings: Peak Force, Slew Rate, and Displacement Sensitivity," ASME J. Tribol., **111**, pp. 331–336.
- [10] Knight, J. D., Xia, E., McCaul, E., and Hacker, Jr., H., 1992, "Determination of Forces in a Magnetic Bearing Actuator: Numerical Computation With Comparison to Experiment," ASME J. Tribol., **114**, pp. 796–801.
- [11] Allaire, P. E., Fittro, R. L., Maslen, E. H., and Wakefield, W. C., 1997, "Measured Force/Current Relations in Solid Magnetic Thrust Bearings," ASME J. Eng. Gas Turbines Power, **119**, pp. 131–142.
- [12] Allaire, P. E., et al., 1988, "Design and Testing of a Magnetic Thrust Bearing," *Proceedings of the NASA Workshop on Magnetic Suspension Technology*.
- [13] Na, U. J., and Palazzolo, A. B., 2000, "Optimized Realization of Fault-Tolerant Heteropolar Magnetic Bearings," ASME J. Vib. Acoust., **122**, pp. 209–221.
- [14] Na, U. J., and Palazzolo, A. B., 2000, "Fault Tolerance of Magnetic Bearings With Material Path Reluctance and Fringing Factors," IEEE Trans Magn., **36**, pp. 3939–3946.
- [15] Keith, F. J., Williams, R. D., and Allaire, P. E., 1990, "Digital Control of Magnetic Bearings Supporting a Multimass Flexible Rotor," STLE Tribol. Trans., **33**, pp. 307–314.